Magnetic-field-induced oscillation of multipartite nonlocality in spin ladders

Hong-Guang Cheng,[1] Meng Li,[1] Yu-Ying Wu,[1] Mei Wang,[1] Duo Zhang,[1] Jia Bao,[2] Bin Guo,[2] and Zhao-Yu Sun[1,*]
[1]*School of Electrical and Electronic Engineering, Wuhan Polytechnic University, Wuhan 430023, China*
[2]*Department of Physics, Wuhan University of Technology, Wuhan 430070, China*

(Received 22 January 2020; accepted 22 April 2020; published 22 May 2020)

Spin-$\frac{1}{2}$ two-leg ladder models under a magnetic field have a well-known phase diagram. In this paper, we use multipartite nonlocality (a measure of multipartite quantum correlations) to characterize the quantum correlations in the ladder models at zero temperature. Both finite-size and infinite-size ladders are considered. We investigate the global nonlocality $\mathcal{S}_g = \mathcal{S}(|\Psi_g\rangle)$, which describes quantum correlations of the ground states $|\Psi_g\rangle$ of the entire lattices, and the partial nonlocality $\mathcal{S}_p = \mathcal{S}(\hat{\rho}_n)$, which describes quantum correlations of the reduced states $\hat{\rho}_n$ of some sublattices in the ladders. We find that as the magnetic field λ increases, the global nonlocality $\mathcal{S}_g$ presents a single-peak curve. Moreover, the logarithmic measure $\ln \mathcal{S}_g$ changes dramatically at the two critical fields λ_{c_1} and λ_{c_2} of the models and thus signals the quantum phase transitions in the models. For the partial nonlocality $\mathcal{S}_p$, in the regions $\lambda_{c_1} < \lambda < \lambda_{c_2}$, we observe that the $\mathcal{S}_p(\lambda)$ curve shows an oscillation. Numerical results reveal that the underling mechanism is the "major component transitions" in the reduced states $\hat{\rho}_n$ of the sublattices. More importantly, the oscillation of the partial nonlocality $\mathcal{S}_p$ is modulated by the single-peak curve of the global nonlocality $\mathcal{S}_g$. The result provides valuable clues about the relation between partial nonlocality and global nonlocality in low-dimensional quantum models.

DOI: 10.1103/PhysRevA.101.052116

I. INTRODUCTION

For decades, concepts established in the field of quantum information have been adopted to investigate other fields of science, such as block holes, quantum chemistry, and particularly, condensed matter physics [1–3]. For instance, based upon a *bipartite* setting of the concerned systems, entanglement entropy [4–7] has been used to investigate quantum phase transitions (QPTs) [8] in various quantum lattices. As a feedback, the obtained knowledge helps us to improve the numerical algorithms for simulating these quantum lattices [9,10].

Recently, much attention has been paid to *multipartite* settings [11–15]. In the field of quantum information, multipartite quantum correlations are regarded as potential resources for quantum communication [2,16]. Moreover, in condensed matter physics, measures of multipartite correlations can reveal the *correlation structure* in many-body quantum systems and help us to gain a deeper insight into condensed matters [17–24].

There are various methods to characterize multipartite quantum correlations. A widely used quantity is multipartite entanglement [14,25–28]. Let us just take a four-party pure state $|\Psi\rangle$, for instance. If $|\Psi\rangle$ can be expressed into a fully separable form $|\psi_1\rangle \otimes |\psi_2\rangle \otimes |\psi_3\rangle \otimes |\psi_4\rangle$, we say that $|\Psi\rangle$ is not entangled. If $|\Psi\rangle$ can be expressed in the form of $|\Psi\rangle = |\psi_{12}\rangle \otimes |\psi_3\rangle \otimes |\psi_4\rangle$ but cannot be expressed into the fully separable form, we will say that $|\Psi\rangle$ is two-partite entangled. If it can be expressed in the form of $|\Psi\rangle = |\psi_{123}\rangle \otimes |\psi_4\rangle$ but cannot be further expressed into any two-partite entangled form, we will say that $|\Psi\rangle$ is three-partite entangled. m-partite entanglement can be defined in a similar way [14]. One can see that multipartite entanglement is always defined based upon some kind of incompatibility with an underlying separable state.

In this paper, we will consider another quantity to characterize multipartite quantum correlations, multipartite nonlocality, which is captured by the violation of multipartite Bell-type inequalities [29–34]. The basic idea for multipartite Bell-type inequalities is as follows. We consider a family of classical communication models $\{m_1, m_2, m_3, \dots\}$. We will calculate the correlations $\{\mathcal{S}_1, \mathcal{S}_2, \mathcal{S}_3, \dots\}$ in these models, and figure out the maximum correlation permitted by this family of models. For a quantum state $\hat{\rho}$, if the Bell-type inequality $\mathcal{S}(\hat{\rho}) \leqslant \max_i \mathcal{S}_i$ is violated, one can conclude that the correlations in $\hat{\rho}$ cannot be reproduced (or simulated) by any of these models. Quantum correlation captured by Bell-type inequalities is usually called *multipartite nonlocality* [33]. With the help of Bell-type inequalities, we can classify general quantum states into a complete set of families, from classical states (which have the lowest hierarchy in the families) to genuine multipartite correlated states (which have the highest hierarchy) [2,17,34]. Moreover, Bell-type inequalities are scalable, that is, they can be applied to arbitrary number of qubits [33] and arbitrary dimensions [34].

Both entanglement and nonlocality are regarded as distinct resources in the field of quantum information. Their difference is that the former is defined on the entanglement-separability paradigm and occurs in Hilbert spaces, while the latter characterizes correlations by analyzing whether they can be reproduced (or simulated) by some predefined classical models (or classical devices) and manifests itself in the ordinary

*Corresponding author: sunzhaoyu2000@qq.com

 ©2020 American Physical Society

$(3+1)$-dimensional space. Some valuable comparisons of these two concepts can be found in Refs. [35,36].

Due to the scalability of Bell-type inequalities and the fast development of the related tensor-network algorithms [21,22,36], Bell-type inequalities and multipartite nonlocality have been used to characterize multisite quantum correlations in various low-dimensional quantum lattices, including the one-dimensional (1D) transverse-field Ising models [18,22,24], 1D *XY* chains [19,20], 1D *XXZ* chains [21], 1D ferromagnetic Heisenberg chains [37], two-dimensional transverse-field Ising lattices [23], N-dimensional Lipkin-Meshkov-Glick models [38,39], and many others [19,36,40,41].

Some broad conclusions have been achieved. First, the nonlocality measure $\mathcal{S}$ shows clear scaling behavior (i.e., $\ln \mathcal{S} \sim N$) for various 1D quantum chains [20–22]. Second, when a QPT occurs, the nonlocality measure usually presents some kind of singularity, which means that the *internal correlation structure* of the ground state changes dramatically in the QPT [19–24,39].

Nevertheless, it is still too early to say that we have established a complete picture about multipartite nonlocality in these low-dimensional quantum systems. Some important fragments of the picture are still missing, for instance, the relation between the *global* nonlocality in the entire lattices and the *partial* nonlocality in n-site sublattices. On one hand, the ground states of quantum models generally contain global nonlocality [18,24,37]. On the other hand, it is rather surprising that for various quantum models [19,41–43], partial nonlocality is absent in two-site sublattices (i.e., $n=2$). It was realized by Oliveira *et al.* that this general conclusion is directly connected to the translational invariance of the models [44,45]. The existence of partial nonlocality was first identified in the *XY* chains with $n \geqslant 4$ [20]. Since then, partial nonlocality with a large n has become a valuable tool to capture multisite quantum correlations in low-dimensional quantum systems and has been used to characterize QPTs in various models [19–24,39]. However, quite recently, it was found that under some situations, when a quantum system exhibits genuine multipartite nonlocality, its subsystems are forbidden to show arbitrarily high nonlocality [46]. This result seems to indicate that, even in the large-n limit, the study of partial nonlocality in the sublattices may not always offer us reliable knowledge about the global nonlocality in the entire systems. Thereby, it becomes important to clarify the relation between global nonlocality and partial nonlocality in these quantum lattices.

In this paper, we will investigate multipartite nonlocality in spin-$\frac{1}{2}$ two-leg ladder models under a magnetic field. The models have a well-known ground-state phase diagram [47]. We will study both the global nonlocality $\mathcal{S}_g$ of the ground states of the entire lattices and the partial nonlocality $\mathcal{S}_p$ of the reduced states of n-rung sublattices in the ladders. We find that as the magnetic field λ increases, the global nonlocality curve $\mathcal{S}_g(\lambda)$ exhibits a *single peak* between the two QPT points λ_{c_1} and λ_{c_2} of the model. In the same regions, nevertheless, the partial nonlocality curve $\mathcal{S}_p(\lambda)$ presents a magnetic-field-induced oscillation. Furthermore, we find numerical evidence that the oscillation of the partial nonlocality is modulated by the *single-peak* curve of the global nonlocality of the model. This result provides an intuitive understanding about the relation between partial nonlocality and global nonlocality in the ladder models.

This paper is organized as follows. In Sec. II the concept of multipartite nonlocality will be reviewed briefly. In Sec. III we will introduce the ladder models. Numerical details in calculating the ground states will also be given. In Sec. IV we will report our results about the global nonlocality of the ground states of the ladders. In Sec. V we move on to discuss the partial nonlocality in consecutive-n-rung sublattices in the middle of the ladders. Finally, a summary and discussion will be given in Sec. VI.

II. BASIC CONCEPTS

Grouping number: An intuitive quantity to characterize the *correlation structure* in many-body systems is the grouping number. Suppose an n-site classical communication model can be divided into g groups, denoted as $\{[1],[2,3,4],[5,6],\ldots,[n]\}$, such that only sites in the same group can communicate with each other. Then the model will be called a g-grouping model [30,32–34]. All these grouping models (with $g=1,2,\ldots,n$) together can reproduce general multipartite correlations. For an n-site quantum state $\hat{\rho}_n$, if its correlations can be reproduced only by grouping models with $g \leqslant g_0$, we say that the grouping number of $\hat{\rho}_n$ is g_0. A state contains genuine multipartite correlations if its grouping number is $g_0(\hat{\rho}_n)=1$ and does not contain any correlation if $g_0(\hat{\rho}_n)=n$. One can see that the grouping number g_0 captures the *internal structure* of multipartite correlations in the state. In practice, g_0 can be detected by Bell-type inequalities.

Mermin-Svetlichny operators: In Bell-type inequalities, the n-site Mermin-Svetlichny (MS) operator plays a central role. The MS operator has a recursive definition [33],

$$\begin{aligned}\hat{M}_{[1\ldots n]} = {} & \tfrac{1}{2}\hat{M}_{[1\ldots n-1]} \otimes (\hat{m}_n + \hat{m}'_n) \\ & + \tfrac{1}{2}\hat{M}'_{[1\ldots n-1]} \otimes (\hat{m}_n - \hat{m}'_n),\end{aligned} \tag{1}$$

where $\hat{m}_n$ and $\hat{m}'_n$ are single-site operators defined as $\hat{m}_n = \boldsymbol{x}_n \cdot \boldsymbol{\sigma}$ and $\hat{m}'_n = \boldsymbol{x}'_n \cdot \boldsymbol{\sigma}$. $\boldsymbol{x}_n$ and $\boldsymbol{x}'_n$ are unit vectors. $\boldsymbol{\sigma} = [\hat{\sigma}_x, \hat{\sigma}_y, \hat{\sigma}_z]$ is the spin vector. The primed operator $\hat{M}'$ is defined in a similar way by exchanging all the $\boldsymbol{x}_j$ and $\boldsymbol{x}'_j$ in $\hat{M}$. Finally, one can see that $\hat{M}_{[1\ldots n]}$ depends on a set of $2n$ unit vectors, $\mathbb{X} = \{\boldsymbol{x}_1, \boldsymbol{x}'_1, \ldots, \boldsymbol{x}_n, \boldsymbol{x}'_n\}$.

Bell-type inequalities: For a quantum state $\hat{\rho}_n$, if the correlations can be reproduced by a g-grouping model, the following Bell-type inequalities should hold [33]:

$$\mathcal{S}(\hat{\rho}_n) = \begin{cases} \max_{\{\mathbb{X}\}} \langle \hat{M}_{[1\ldots n]}(\mathbb{X}) \rangle \leqslant 2^{\frac{n-g}{2}}, & \text{for n-g even}, \\ \max_{\{\mathbb{X}\}} \langle \hat{M}^{+}_{[1\ldots n]}(\mathbb{X}) \rangle \leqslant 2^{\frac{n-g}{2}}, & \text{for n-g odd}, \end{cases} \tag{2}$$

where $\hat{M}^{+}_{[1\ldots n]} = \frac{1}{\sqrt{2}}(\hat{M}_{[1\ldots n]} + \hat{M}'_{[1\ldots n]})$, and $\langle\cdot\rangle$ denotes the standard expectation value for the state $\hat{\rho}_n$. The inequality is defined for general quantum states. For a pure state $|\Psi\rangle$, the LHS of Eq. (2) can be rephrased as $\mathcal{S}(|\Psi\rangle\langle\Psi|)$.

If Eq. (2) is violated, one can conclude that (at most) $[g-1]$-grouping models are needed to reproduce the multipartite correlations in $\hat{\rho}_n$. Thereby Bell-type inequalities can be used to calculate the *upper bound* of the grouping number of the state. In the literature, multipartite correlation identified

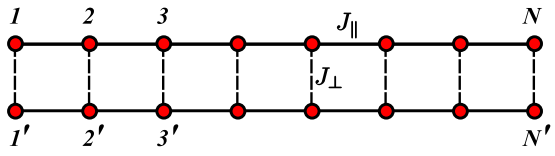

FIG. 1. Lattice structure of the two-leg ladders with open boundary conditions. N denotes the length of the ladders. $J_{||}$ and $J_{\perp}$ describe the exchange interactions along the legs and the rungs, respectively.

by the violation of Bell-type inequalities is usually called "multipartite nonlocality." It is clear that a higher (lower) value of the measure $\mathcal{S}$ indicates a smaller (larger) value of the grouping number and, consequently, a higher (lower) hierarchy of multipartite nonlocality. Furthermore, in low-dimensional quantum systems, we are usually just interested in the qualitative behavior of multipartite nonlocality, rather than the specific value of the grouping number. Thereby, for Eq. (2), we will ignore the parity of $n-g$ and just consider the first inequality.

Two-site update algorithm: The optimization of the nonlocality measure $\mathcal{S}(\hat{\rho}_n)$ is highly nontrivial. In this paper we will use the two-site update algorithm to carry out the optimization, which was first proposed in Ref. [22]. In the algorithm, based upon a tripartite form of the MS operator, the n-site optimization problem involved in Eq. (2) is transformed into a series of two-site optimizations, and thus the numerical efficiency is dramatically improved. For the details of the algorithm, readers are referred to Ref. [22].

III. MODELS AND METHODS

The two-leg spin ladders under a magnetic field can be described by the following Hamiltonian [47]:

$$\hat{\mathcal{H}}_0 = J_{||}\sum_{i=1}^{N-1}(\mathbf{S}_i\cdot\mathbf{S}_{i+1}+\mathbf{S}_{i'}\cdot\mathbf{S}_{(i+1)'}) + J_{\perp}\sum_{i=1}^{N}\mathbf{S}_i\cdot\mathbf{S}_{i'} - \lambda\sum_{i=1}^{N}\left(\hat{S}_i^z+\hat{S}_{i'}^z\right). \quad (3)$$

The lattice structure of the models is shown in Fig. 1. $J_{||}>0$ and $J_{\perp}>0$ are the antiferromagnetic nearest-neighboring coupling constants on the legs and the rungs, respectively. λ denotes the strength of the magnetic field along the z direction. i and i' denote sites on the upper leg and the lower leg, respectively. $\mathbf{S}_{i(')}$ and $\hat{S}_{i(')}^z$ are the standard spin vector and spin operator, respectively. We just consider open boundary conditions in this paper.

Moreover, without loss of generality, in this paper we will use $J_{||}$ to rescale the parameters in Eq. (3) as $\frac{J_{||}}{J_{||}}\to 1$, $\frac{J_{\perp}}{J_{||}}\to J_{\perp}$, and $\frac{\lambda}{J_{||}}\to\lambda$. Thereby, the rescaled Hamiltonian will be governed by just two quantities:

$$\hat{\mathcal{H}} = \sum_{i=1}^{N-1}(\mathbf{S}_i\cdot\mathbf{S}_{i+1}+\mathbf{S}_{i'}\cdot\mathbf{S}_{(i+1)'}) + J_{\perp}\sum_{i=1}^{N}\mathbf{S}_i\cdot\mathbf{S}_{i'} - \lambda\sum_{i=1}^{N}\left(\hat{S}_i^z+\hat{S}_{i'}^z\right). \quad (4)$$

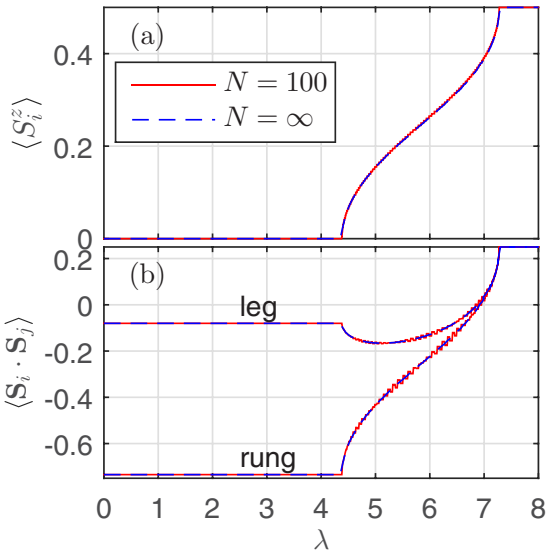

FIG. 2. (a) Magnetization and (b) nearest-neighboring correlations in the ladder models (with $J_{\perp}/J_{||}=5.28$) as a function of λ. λ is a dimensionless quantity describing the rescaled strength of the magnetic field [see Eq. (4)]. Two critical points locate at $\lambda_{c_1}=4.38$ and $\lambda_{c_2}=7.28$. The red solid lines correspond to ladders with $N=100$ (calculated by ALPS package [48]), and the blue dashed lines correspond to infinite-size ladders (calculated with the Matrix-Product Toolkit [49]).

Both $J_{\perp}$ and λ become dimensionless. Alternatively, we can also say that they are in the unit of $J_{||}$.

When the magnetic field is absent (i.e., $\lambda=0$), the ground state is a gapped, disordered quantum spin liquid [47,50,51]. It is quite intuitive to consider the $J_{\perp}\to\infty$ limit, where the ladder reduces into N uncoupled rungs. One can see that the ground state is just a spin singlet, which has a finite energy gap with the triplet excited states. For ladders with any finite positive $J_{\perp}$, the energy gap survives [52] and will be denoted as Δ.

When the strength λ of the magnetic field increases, according to Eq. (4), the energy of the singlet state would keep unchanged, and the energy for a triplet state would be reduced linearly [53]. Thereby, at some magnetic field λ_{c_1}, the energy gap would be closed, and there is a transition from the nonmagnetic ground state to a gapless Luttinger liquid phase [47,50]. The magnetization increases gradually when $\lambda>\lambda_{c1}$. At a strong enough magnetic field λ_{c_2}, the ground state becomes a fully polarized state and a finite energy gap would be open again [54]. Both λ_{c_1} and λ_{c_2} are the quantum critical points of the models [50,51,54,55], and the transitions at the two points are second-order QPTs. Previous studies show that in the thermodynamic limit, the magnetization would show square-root singularities at λ_{c_1} and λ_{c_2} [47]. Moreover, in the vicinity of these two critical points, the magnetization obeys a universal scaling function [50].

The two critical points locate at $\lambda_{c1}=\Delta$ and $\lambda_{c2}=J_{\perp}+2$ [47]. In addition, the full magnetic phase diagram of the ladder models on the $\lambda\sim J_{\perp}$ plane can be found in Ref. [56]. According to the phase diagram, the value of $J_{\perp}$ just affects the phase boundaries and does not change the fundamental physics of the ground states. Thereby, in this paper we will just

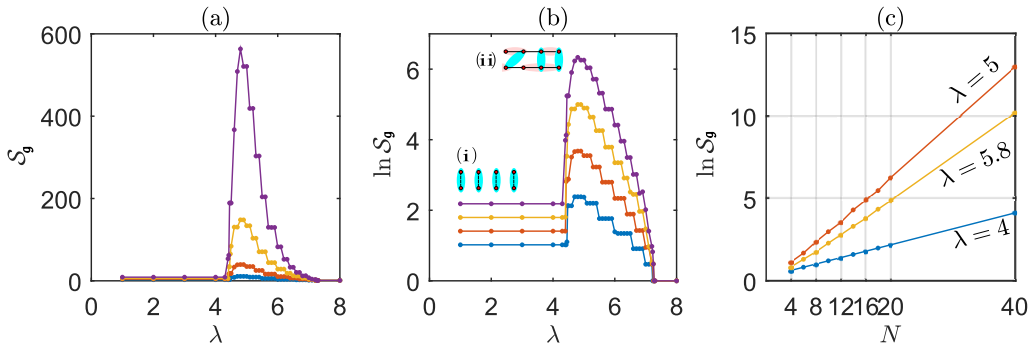

FIG. 3. (a) Global nonlocality $\mathcal{S}_g = \mathcal{S}(|\Psi_g\rangle)$ for the ground states $|\Psi_g\rangle$ of finite-size ladders as a function of the magnetic field λ. From bottom to top, the curves correspond to $N = 8, 12, 16, 20$, respectively. (b) Logarithmic measure $\ln \mathcal{S}_g$. The insets (i) and (ii) illustrate intuitively how nonlocality spreads in the lattices for $\lambda < \lambda_{c_1}$ and $\lambda_{c_1} < \lambda < \lambda_{c_2}$, respectively. They explain why $\mathcal{S}_g$ changes dramatically at λ_{c_1} (and similarly, at λ_{c_2}). (c) Linear scaling of the logarithmic measure $\ln \mathcal{S}_g$ for several fixed magnetic fields. Panels (b) and (c) together offer us a clear picture for the global nonlocality in the large-N limit.

consider the coupling parameter $J_\perp = 5.28$, which has been used to model the real material $Cu_2(C_5H_{12}N_2)_2Cl_4$ [47,57]. It is expected that the phenomenon reported in this paper shall be observed in ladders with any finite positive $J_\perp$.

First, we shall use numerical methods to figure out the ground-state wave functions of the ladders. We will consider both finite-size ladders and infinite-size ladders. For the first situations, we will use the "mps-optim" package in the Algorithms and Libraries for Physics Simulations (ALPS) project [48] to figure out the ground states, with N up to 100. We set the max number of states as $m = 200$ and sweep the lattices 30–50 times. For the second situations, we will use the Matrix-Product (MP) Toolkit [49] to calculate the ground states, with the max number of states $m = 200$. The average magnetization and nearest-neighboring two-spin correlations are shown in Fig. 2. The critical points are $\lambda_{c_1} = 4.38$ and $\lambda_{c_2} = 7.28$, which are quite consistent with previous results [47]. Thereby, our numerical wave functions are quite reliable.

After figuring out the wave functions, the nonlocality measure $\mathcal{S}$ defined in Eq. (2) will be optimized with the above mentioned two-site update algorithm [22]. To improve the reliability of the optimization, for each set of physical parameters, we will randomly generate $r = 30$ initial points, and carry out r rounds of optimization independently. The best result in these r rounds would be used as the final optimization result. In subsequent sections, we will report our results about the global nonlocality of the ground states of the entire ladders and the partial nonlocality of the reduced density matrices of consecutive-n-rungs sublattices in the middle of the ladders.

IV. GLOBAL NONLOCALITY IN ENTIRE LATTICE

The global nonlocality $\mathcal{S}_g = \mathcal{S}(|\Psi_g\rangle)$ for the ground states $|\Psi_g\rangle$ of infinite-size ladders cannot be calculated directly. Thereby, we will consider finite-size ladders and try to capture the large-N behavior by finite-size scaling analysis.

In Fig. 3(a) we have shown the nonlocality measure $\mathcal{S}_g$ as a function of the magnetic field λ with $N = 8, 12, 16$, and 20. In the gapped phase $\lambda < \lambda_{c_1}$, $\mathcal{S}_g$ keeps constant for any N. Moreover, in the fully polarized phase $\lambda > \lambda_{c_2}$, we always have $\mathcal{S}_g = 1$. In the phase $\lambda_{c_1} < \lambda < \lambda_{c_2}$, as λ increases, the nonlocality measure first shows a sharp increase, then achieves a peak, and finally decreases to 1.

We have also illustrate the logarithmic measure $\ln \mathcal{S}_g$ in Fig. 3(b). We find that with the increase of N, the $\ln \mathcal{S}_g(\lambda)$ curve rises evenly, which offers a strong hint about what will happen in the limit $N \to \infty$. Furthermore, for several typical λ, we have carried out scaling analysis with N up to 40, and the results are shown in Fig. 3(c). One can see clearly that for any fixed λ, the logarithmic measure $\ln \mathcal{S}_g$ would be a linear function of N when N is large enough.

Finally, we shall draw a physical picture about the global nonlocality in the entire magnetic-field regions. First, in the gapped phase $\lambda < \lambda_{c_1}$, since $J_\perp = 5.28$ is quite large, the ground state may be described approximately by a rung-product state,

$$|\Psi^{\text{gap}}\rangle \approx \prod_{i=1}^{N} |\varphi_i^{\text{rung}}\rangle, \tag{5}$$

where $|\varphi_i^{\text{rung}}\rangle$ denotes the ground state of the ith isolated rung. It is expected that nonlocality spreads mainly in each rung, rather than along the legs [the behavior is illustrated in inset (i) of Fig. 3(b)]. Consequently, the multipartite nonlocality measure $\mathcal{S}_g$ takes a relatively low value when $\lambda < \lambda_{c_1}$. When the magnetic field crosses the critical point λ_{c_1}, the rung-product state $|\Psi^{\text{gap}}\rangle$ is destroyed, and nonlocality can spread along the two legs [see inset (ii) in Fig. 3(b)]. Thereby, $\ln \mathcal{S}_g$ increases rapidly and its first-order derivative is divergent at $\lambda = \lambda_{c_1}$. One can see that the dramatic change of $\ln \mathcal{S}_g$ at $\lambda = \lambda_{c_2}$ can be explained in a similar way. Let us begin with a strong magnetic field $\lambda > \lambda_{c_2}$, for which the ground state is the fully polarized state

$$|\Psi^{\uparrow}\rangle = \prod_{i=1}^{N} |\uparrow\uparrow\rangle. \tag{6}$$

This state is a classical state, and no nonlocality could spread in the rungs or along the legs. When the magnetic field decreases gradually and finally crosses the critical point λ_{c_2}, the state $|\Psi^{\uparrow}\rangle$ is destroyed, and nonlocality can spread both in the rungs and along the legs. That is why $\ln \mathcal{S}_g$ increases rapidly at $\lambda = \lambda_{c_2}$.

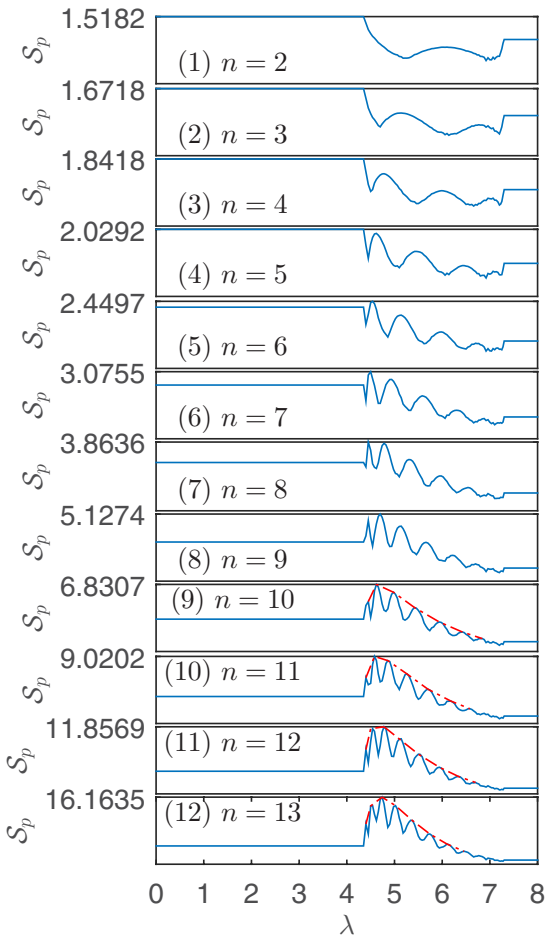

FIG. 4. Partial nonlocality $\mathcal{S}_p = \mathcal{S}(\hat{\rho}_n)$ of the reduced states $\hat{\rho}_n$ for consecutive-n-rung sublattices in infinite-size ladders. $\mathcal{S}_p$ presents a magnetic-field-induced multipeak oscillation in the regions $\lambda_{c_1} < \lambda < \lambda_{c_2}$. When n is large enough, the $\mathcal{S}_p(\lambda)$ curve exhibits a clear single-peak envelope (the red dashed lines). The single-peak envelope suggests that the behavior of partial nonlocality in the sublattices is modulated by the behavior of the global nonlocality in the entire lattice [see the curve of $\mathcal{S}_g(\lambda)$ in Fig. 3].

V. PARTIAL NONLOCALITY IN SUBLATTICES

In this section we will investigate the partial nonlocality in some sublattices in the models. The entire ladders are still in their ground states $|\Psi_g\rangle$. The concerned sublattices consist of n continuous rungs in the middle of the ladders. The reduced density matrices $\hat{\rho}_n$ of these sublattices are obtained by taking a *partial* trace with respect to all the degrees of freedom of its environment, $\hat{\rho}_n = \mathrm{Tr}_{\overline{[1\ldots n]}}|\Psi_g\rangle\langle\Psi_g|$. Both infinite-size ladders and finite-size ladders are considered.

For infinite-size ladders, our main results of the partial nonlocality $\mathcal{S}(\hat{\rho}_n)$ are present in Fig. 4, with $n = 2, 3, 4, \ldots, 13$. First, for $\lambda < \lambda_{c_1}$ and $\lambda > \lambda_{c_2}$, the nonlocality measure keeps constant, which is similar to the global nonlocality $\mathcal{S}(|\Psi_g\rangle)$ in Fig. 3. Nevertheless, for $\lambda_{c_1} < \lambda < \lambda_{c_2}$, partial nonlocality presents a peculiar oscillation. When $n = 2$, one can find a round peak in the $\mathcal{S}_p(\lambda)$ curve [see Fig. 4(1)]. For $n = 3$, two peaks are observed [see Fig. 4(2)]. As n increases, the number of peaks increases steadily, and $\mathcal{S}_p$ presents a multipeak oscillation behavior. We take $n = 13$ as an example and use the Bell-type inequalities in Eq. (2) to analyze the grouping number of the reduced state $\hat{\rho}_n$. When the magnetic field increases gradually from λ_{c_1} to λ_{c_2}, the grouping number of $\hat{\rho}_n$ also oscillates and takes in succession the value of 19, 21, 19, 17, 19, 21, 19, 21, 23, 21, 23, 25, 23, and 25. Furthermore, when n is large enough, we find that the $\mathcal{S}_p(\lambda)$ curve exhibits a clear envelope curve [the red dashed line in Fig. 4(9)–(12)]. One can see that the envelope curve is a single-peak curve.

Before investigating the multipeak oscillation behavior in detail, we will offer a phenomenological explanation about the single-peak envelope curve of $\mathcal{S}_p(\lambda)$. First, in infinite-size ladders, the entire lattices consist of three blocks: the left semi-infinite environment block, the concerned n-rung sublattices, and the right semi-infinite environment block. It is clear that even in the large-n limit, the reduced states $\hat{\rho}_n$ would not be equivalent to the ground states $|\Psi_g\rangle$. Nevertheless, when n is large enough, we still expect that the partial nonlocality $\mathcal{S}_p$ of the sublattices should *inherit* some of the features of the global nonlocality $\mathcal{S}_g$ of the entire lattices. As is shown in Fig. 3, the global nonlocality curve is a single-peak curve. Thereby, a physical explanation of the single-peak envelope curve of $\mathcal{S}_p(\lambda)$ is that, in the large-n limit, the partial nonlocality of the sublattices is *modulated* by the global nonlocality of the entire lattice.

We turn to investigate the multipeak feature in the partial nonlocality. First, we have carefully rechecked our numerical results by considering finite-size ladders with $N = 100$. With the help of the conserved-quantum-number technique, we are able to diagonalize the Hamiltonian in each S^z_{total} sector, which greatly improves the convergence of the wave functions [48]. The final result is illustrated with red dots in Fig. 5(a1)–(a4).[1] The result for $N = \infty$ is also shown with blue circles for comparison. In the vicinity of λ_{c_2}, the curves for $N = \infty$ show slight fluctuations, which result from imperfect convergence of the wave functions. For the finite-size ladders, where the convergence of the wave functions is much better, the curves are quite smooth. Finally, the qualitative consistence of the two results ensures that the multipeak oscillation of the partial nonlocality is indeed an intrinsic feature in the ladder models.

To figure out the origin of the oscillation, with the help of the eigenvalue decomposition we have carried out a component analysis of the reduced density matrices $\hat{\rho}_n$ as

$$\hat{\rho}_n = \sum_i \omega_i |\psi_i\rangle\langle\psi_i|, \tag{7}$$

where $|\psi_i\rangle$ are the components of $\hat{\rho}_n$ and ω_i are the corresponding weights. In Fig. 5(b1)–(b4) we have illustrated the weights ω_i of these components as a function of the magnetic field.

First, two components need to be explained separately. One is connected to the rung-product state $|\Psi^{\mathrm{gap}}\rangle$ in Eq. (5) and is marked as $|\psi_{\mathrm{rung}}\rangle$ in Fig. 5(b1)–(b4). The other one is connected to the fully polarized state $|\Psi^{\uparrow}\rangle$ in Eq. (6) and is

[1]Only results for $S^z_{\mathrm{total}} = 0, 2, 4, \ldots, N$ have been shown in Fig. 5. For finite-size ladders, there is a small even-odd effect in the $\mathcal{S}_p(\lambda)$ curves.

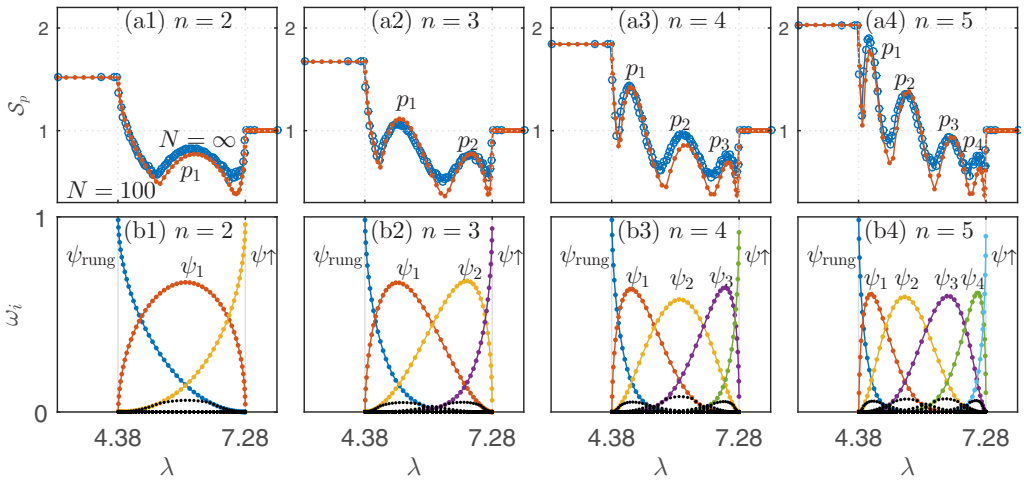

FIG. 5. Partial nonlocality $\mathcal{S}_p = \mathcal{S}(\hat{\rho}_n)$ of the reduced states $\hat{\rho}_n$ for consecutive-n-rung sublattices in the middle of an N-rung ladder with total length $N = 100$ (red dots) and various n: (a1) $n = 2$, (a2) $n = 3$, (a3) $n = 4$, and (a4) $n = 5$. Results for $N \to \infty$ (blue circles) are also shown for a comparison purpose. (b1)–(b4) The results of the component analysis of the reduced density matrices $\hat{\rho}_n$, $\hat{\rho}_n \to \sum_i \omega_i |\psi_i\rangle\langle\psi_i|$, where ω_i denotes the weight of the component $|\psi_i\rangle$. As the magnetic field increases, these components take turns serving as the *major component* (i.e., the component which has the largest weight) of $\hat{\rho}_n$. The peaks of ω_i of the *major components* and the peaks of $\mathcal{S}_p$ have an one-to-one correspondence and exhibit quite similar morphology. It suggests that the multipeak oscillation of the partial nonlocality originates from the "major component transitions" in $\hat{\rho}_n$.

marked as $|\psi_\uparrow\rangle$. For $\lambda < \lambda_{c_1}$ and $\lambda > \lambda_{c_2}$, the reduced state $\hat{\rho}_n$ is equivalent to $|\psi_{\text{rung}}\rangle$ and $|\psi_\uparrow\rangle$, respectively. Thereby, when λ increases from λ_{c_1} to λ_{c_2}, the weight of $|\psi_{\text{rung}}\rangle$ decreases monotonically from 1 to 0, and the weight of $|\psi_\uparrow\rangle$ increases monotonically from 0 to 1.

Next, we pay our attention to other components. In the regions $\lambda \leqslant \lambda_{c_1}$ and $\lambda \geqslant \lambda_{c_2}$, the weights ω_i of these components are simply zero. Thereby, when λ increases from λ_{c_1} to λ_{c_2}, ω_i would experience a process of first increasing and then decreasing. As can be seen in the figures, the weight of each of these components indeed shows a round peak.

Finally, let us focus on some special components of $\hat{\rho}_n$, the *major components*. For a fixed λ, suppose a component $|\psi_{i_0}\rangle$ has the largest weight,

$$\omega_{i_0} = \max_i \{\omega_i\}.$$

We will say that $|\psi_{i_0}\rangle$ is the *major component* of $\hat{\rho}_n$. Let us take $n = 3$ in Fig. 5(b2) as an example. When the magnetic field increases from λ_{c_1} to λ_{c_2}, the components $|\psi_{\text{rung}}\rangle$, $|\psi_1\rangle$, $|\psi_2\rangle$, and $|\psi_\uparrow\rangle$ take turns serving as the major component of $\hat{\rho}_n$. In the magnetic field region where some $|\psi_{i_0}\rangle$ is the major component, the quantum correlations in $\hat{\rho}_n$ would be determined mainly by $|\psi_{i_0}\rangle$ and its weight ω_{i_0}.

In Fig. 5, by comparing the peaks of $\mathcal{S}_p$ (marked as p_k in the figure) and the peaks of the weights of the major components, one can see that both the location and the morphology of the two are quite similar. This feature helps us to figure out the origin of the oscillation of the partial nonlocality. We take the major component $|\psi_1\rangle$ in Fig. 5(b2) as an example. At the magnetic field where the weight of $|\psi_1\rangle$ (ω_1) achieves its peak value, one can see that the weights for other components are quite small. Thereby, it is expected that in the vicinity of the peak, $|\psi_1\rangle$ and its weight ω_1 would largely determine the value of $\mathcal{S}_p(\hat{\rho}_n)$. When ω_1 shows a peak, the partial nonlocality $\mathcal{S}_p$ will also present a peak. In this way, each major component $|\psi_{i_0}\rangle$ (except $|\psi_{\text{rung}}\rangle$ and $|\psi_\uparrow\rangle$) would contribute a peak in the $\mathcal{S}_p(\lambda)$ curve. Finally, we can conclude that the underling mechanism of the oscillation in the partial nonlocality $\mathcal{S}_p$ is the "major component transitions" in the density matrices $\hat{\rho}_n$ of the sublattices.

VI. SUMMARY AND DISCUSSION

In this paper, we have investigated spin-$\frac{1}{2}$ two-leg ladder models under a magnetic field, which have a rich ground-state phase diagram. We have used multipartite nonlocality to characterize the influence of the magnetic field λ on the quantum correlations in the models. For such a purpose, we have consider two measures. The first one is the global nonlocality $\mathcal{S}_g = \mathcal{S}(|\Psi_g\rangle)$, which captures quantum correlations in the ground states of the entire lattices. The second one is the partial nonlocality $\mathcal{S}_p = \mathcal{S}(\hat{\rho}_n)$, which captures quantum correlations in the reduced density matrices $\hat{\rho}_n$ of n-rung sublattices in the ladders. Both finite-size and infinite-size ladders have been considered.

For the global nonlocality $\mathcal{S}_g$, we have mainly considered finite-size ladders (with length N), and tried to capture the large-N behavior with finite-size scaling analysis. For any fixed magnetic field, when N is large enough, $\ln \mathcal{S}_g$ is a linear function of N. Combined with the scaling behavior and some qualitative analysis of the ground states, we have drawn a reliable picture for the global nonlocality in the large-N limit, that is, $\ln \mathcal{S}_g(\lambda)$ would exhibit a single-peak curve between the critical points λ_{c_1} and λ_{c_2}. Moreover, its first-order derivative would be divergent in the vicinity of the two critical points. It means that the *correlation structure* of the ground states changes sharply in the vicinity of the QPT points of the ladders.

Our second observation is about the partial nonlocality $\mathcal{S}_p$ in the sublattices (with length n) in both finite-size ladders

and infinite-size ladders. When n is large enough, we find that the partial nonlocality $\mathcal{S}_p$ exhibits a magnetic-field-induced multipeak oscillation, and the envelope curve of the oscillation is a single-peak curve.

The single-peak structure in the envelope curve of $\mathcal{S}_p(\lambda)$ shows that the partial nonlocality of the sublattices is modulated by the global nonlocality of the entire lattice, where the latter has a single-peak feature. The underlying mechanics is that when n is large enough, partial nonlocality in the sublattices should *inherit* some of the features of the global nonlocality in the entire lattices.

Numerical results reveal that the physical origin of the multipeak oscillation in $\mathcal{S}_p(\lambda)$ is the "major component transitions" in the reduced states $\hat{\rho}_n$ of the sublattices. We have carried out a component analysis of $\hat{\rho}_n$ as $\hat{\rho}_n = \sum_i \omega_i |\psi_i\rangle\langle\psi_i|$. As the magnetic field increases, different components $|\psi_i\rangle$ take turns serving as the major component of $\hat{\rho}_n$. Consequently, the leading weight, $\omega_{i_0}(\lambda) = \max_i\{\omega_i(\lambda)\}$, shows several peaks in Fig. 5. In the vicinity of each peak of ω_{i_0}, the weights for other components are quite small, and thus the behavior of $\mathcal{S}_p(\hat{\rho}_n)$ would be largely determined by ω_{i_0}. When ω_{i_0} shows a peak, the partial nonlocality $\mathcal{S}_p$ would also present a peak. In this way, each major component $|\psi_{i_0}\rangle$ would contribute a peak in the $\mathcal{S}_p(\lambda)$ curve, and the "major component transitions" in the density matrices $\hat{\rho}_n$ would result in an oscillation in the partial nonlocality $\mathcal{S}_p$.

It may be interesting to compare the major-component transitions (MCTs) in the density matrices and the quantum phase transitions (QPTs) in the ground states of the ladder models. QPTs occur at the crossing point between the *lowest*-lying energy levels of the systems, and MCTs occur at the crossing point between the *highest* weighted components of the density matrices $\hat{\rho}_n$. For the ladder models considered in this paper, the QPTs result in dramatic changes of the global nonlocality $\mathcal{S}_g$ in the vicinity of the critical points λ_{c_1} and λ_{c_2} (see Fig. 3), and the MCTs result in a multipeak oscillation of the partial nonlocality $\mathcal{S}_p$ in the regions $\lambda_{c_1} < \lambda < \lambda_{c_2}$ (see Figs. 4 and 5).

The numerical results in this paper provide valuable clues about the relation between partial nonlocality and global nonlocality in low-dimensional quantum models. We would like to mention that some other models, such as the one-dimensional diamond chains, also have a quite nontrivial phase diagram and have been realized in real materials [56,58]. It may be interesting to analyze partial nonlocality and global nonlocality in these models and verify the modulation relation between the global nonlocality and the partial nonlocality reported in this paper.

ACKNOWLEDGMENTS

We would like to thank Prof. Ian McCulloch for helpful suggestions about the usage of the Matrix-Product Toolkit. The research was supported by the National Natural Science Foundation of China (Grant Nos. 11675124 and 11704295). H.-G.C. was also supported by the Research Project of the Hubei Provincial Department of Education, China (Grant No. Q20161708).

[1] G. Adesso, T. R. Bromley, and M. Cianciaruso, J. Phys. A: Math. Theor. **49**, 473001 (2016).
[2] G. D. Chiara and A. Sanpera, Rep. Prog. Phys. **81**, 074002 (2018).
[3] R. Horodecki, P. Horodecki, M. Horodecki, and K. Horodecki, Rev. Mod. Phys. **81**, 865 (2009).
[4] A. Osterloh, L. Amico, G. Falci, and R. Fazio, Nature (London) **416**, 608 (2002).
[5] G. Vidal, J. I. Latorre, E. Rico, and A. Kitaev, Phys. Rev. Lett. **90**, 227902 (2003).
[6] L.-A. Wu, M. S. Sarandy, and D. A. Lidar, Phys. Rev. Lett. **93**, 250404 (2004).
[7] D. Larsson and H. Johannesson, Phys. Rev. Lett. **95**, 196406 (2005).
[8] S. Sachdev, *Quantum Phase Transitions* (Cambridge University Press, Cambridge, 1999).
[9] S. R. White, Phys. Rev. Lett. **69**, 2863 (1992).
[10] R. Orús, Ann. Phys. **349**, 117 (2014).
[11] X. Wang, C. Zhang, Q. Chen, S. Yu, H. Yuan, and C. H. Oh, Phys. Rev. A **94**, 022110 (2016).
[12] S. Raeisi, P. Kurzyński, and D. Kaszlikowski, Phys. Rev. Lett. **114**, 200401 (2015).
[13] J.-D. Bancal, J. Barrett, N. Gisin, and S. Pironio, Phys. Rev. A **88**, 014102 (2013).
[14] F. Levi and F. Mintert, Phys. Rev. Lett. **110**, 150402 (2013).
[15] C. C. Rulli and M. S. Sarandy, Phys. Rev. A **84**, 042109 (2011).
[16] V. Scarani and N. Gisin, Phys. Rev. Lett. **87**, 117901 (2001).
[17] O. Gühne, G. Tóth, and H. J. Briegel, New J. Phys. **7**, 229 (2005).
[18] S. Campbell and M. Paternostro, Phys. Rev. A **82**, 042324 (2010).
[19] J. Batle and M. Casas, Phys. Rev. A **82**, 062101 (2010).
[20] Z.-Y. Sun, Y.-Y. Wu, J. Xu, H.-L. Huang, B.-F. Zhan, B. Wang, and C.-B. Duan, Phys. Rev. A **89**, 022101 (2014).
[21] Z.-Y. Sun, S. Liu, H.-L. Huang, D. Zhang, Y.-Y. Wu, J. Xu, B.-F. Zhan, H.-G. Cheng, C.-B. Duan, and B. Wang, Phys. Rev. A **90**, 062129 (2014).
[22] Z.-Y. Sun, B. Guo, and H.-L. Huang, Phys. Rev. A **92**, 022120 (2015).
[23] Z.-Y. Sun, X. Guo, and M. Wang, Eur. Phys. J. B **92**, 75 (2019).
[24] Z.-Y. Sun, M. Wang, Y.-Y. Wu, and B. Guo, Phys. Rev. A **99**, 042323 (2019).
[25] T. R. de Oliveira, G. Rigolin, M. C. de Oliveira, and E. Miranda, Phys. Rev. Lett. **97**, 170401 (2006).
[26] T. R. de Oliveira, G. Rigolin, M. C. de Oliveira, and E. Miranda, Phys. Rev. Lett. **98**, 079902(E) (2007).
[27] H. He and G. Vidal, Phys. Rev. A **91**, 012339 (2015).
[28] A. Bayat, Phys. Rev. Lett. **118**, 036102 (2017).
[29] J. S. Bell, Phys. Phys. Fiz. **1**, 195 (1964).
[30] D. Collins, N. Gisin, S. Popescu, D. Roberts, and V. Scarani, Phys. Rev. Lett. **88**, 170405 (2002).
[31] Q. Y. He, E. G. Cavalcanti, M. D. Reid, and P. D. Drummond, Phys. Rev. Lett. **103**, 180402 (2009).
[32] N. Brunner, J. Sharam, and T. Vértesi, Phys. Rev. Lett. **108**, 110501 (2012).

[33] J.-D. Bancal, C. Branciard, N. Gisin, and S. Pironio, Phys. Rev. Lett. **103**, 090503 (2009).
[34] J.-D. Bancal, N. Brunner, N. Gisin, and Y.-C. Liang, Phys. Rev. Lett. **106**, 020405 (2011).
[35] E. A. Fonseca and F. Parisio, Phys. Rev. A **92**, 030101(R) (2015).
[36] Z. Wang, S. Singh, and M. Navascués, Phys. Rev. Lett. **118**, 230401 (2017).
[37] Y. Dai, C. Zhang, W. You, Y. Dong, and C. H. Oh, Phys. Rev. A **96**, 012336 (2017).
[38] F. Altintas and R. Eryigit, Ann. Phys. **327**, 3084 (2012).
[39] J. Bao, B. Guo, H.-G. Cheng, M. Zhou, J. Fu, Y.-C. Deng, and Z.-Y. Sun, Phys. Rev. A **101**, 012110 (2020).
[40] B.-J. Chen, Z.-Y. Sun, H.-L. Huang, and B. Wang, Eur. Phys. J. B **87**, 282 (2014).
[41] H.-L. Huang, Z.-Y. Sun, and B. Wang, Eur. Phys. J. B **86**, 279 (2013).
[42] L. Justino and T. R. de Oliveira, Phys. Rev. A **85**, 052128 (2012).
[43] D.-L. Deng, C. Wu, J.-L. Chen, S.-J. Gu, S. Yu, and C. H. Oh, Phys. Rev. A **86**, 032305 (2012).
[44] T. R. de Oliveira, A. Saguia, and M. S. Sarandy, Europhys. Lett. **100**, 60004 (2012).
[45] Z.-Y. Sun, Y.-Y. Wu, J. Xu, H.-L. Huang, B.-J. Chen, and B. Wang, Phys. Rev. A **88**, 054101 (2013).
[46] S. Sami, I. Chakrabarty, and A. Chaturvedi, Phys. Rev. A **96**, 022121 (2017).
[47] X. Wang and L. Yu, Phys. Rev. Lett. **84**, 5399 (2000).
[48] B. Bauer, L. D. Carr, H. G. Evertz, A. Feiguin, J. Freire, S. Fuchs, L. Gamper, J. Gukelberger, E. Gull, S. Guertler *et al.*, J. Stat. Mech.: Theory Exp. (2011) P05001.
[49] I. P. McCulloch and M. Gulácsi, Europhys. Lett. **57**, 852 (2002).
[50] B. C. Watson, V. N. Kotov, M. W. Meisel, D. W. Hall, G. E. Granroth, W. T. Montfrooij, S. E. Nagler, D. A. Jensen, R. Backov, M. A. Petruska *et al.*, Phys. Rev. Lett. **86**, 5168 (2001).
[51] S. Wessel, M. Olshanii, and S. Haas, Phys. Rev. Lett. **87**, 206407 (2001).
[52] D. G. Shelton, A. A. Nersesyan, and A. M. Tsvelik, Phys. Rev. B **53**, 8521 (1996).
[53] M. Usami and S.-I. Suga, Phys. Rev. B **58**, 14401 (1998).
[54] R. Chitra and T. Giamarchi, Phys. Rev. B **55**, 5816 (1997).
[55] S. Sachdev, Science **288**, 475 (2000).
[56] D. C. Cabra, A. Honecker, and P. Pujol, Phys. Rev. Lett. **79**, 5126 (1997).
[57] G. Chaboussant, P. A. Crowell, L. P. Lévy, O. Piovesana, A. Madouri, and D. Mailly, Phys. Rev. B **55**, 3046 (1997).
[58] H. Kikuchi, Y. Fujii, M. Chiba, S. Mitsudo, T. Idehara, T. Tonegawa, K. Okamoto, T. Sakai, T. Kuwai, and H. Ohta, Phys. Rev. Lett. **94**, 227201 (2005).